Chemical Engineering Journal 149 (2009) 363–369

Contents lists available at ScienceDirect

Chemical Engineering Journal

journal homepage: www.elsevier.com/locate/cej

Analysis and modeling of adiabatic reactor for monoethanolamine selective production

Hideaki Tsuneki[a,*], Atsushi Moriya[b]

[a] R&D Division, Nippon Shokubai Co., Ltd., 5-8 Nishiotabicho, Suita, Osaka 564-8512, Japan
[b] Himeji Plant, Nippon Shokubai Co., Ltd., 992-1 Aza Nishioki Okihama, Aboshi-ku Himeji, Hyogo 671-1282, Japan

ARTICLE INFO

Article history:
Received 5 May 2008
Received in revised form 2 December 2008
Accepted 3 December 2008

Keywords:
Monoethanolamine
Ethylene oxide
Heat capacity
Adiabatic reactor

ABSTRACT

Ethanolamines are important basic chemicals, and a heat resistant catalyst having high selectivity and activity has been required for producing monoethanolamine and diethanolamine in larger amounts to satisfy the increasing demands. Nippon Shokubai developed a modified clay catalyst for selective monoethanolamine production. The heat capacity of a multicomponent system (ammonia, ethylene oxide, and ethanolamines) was measured with pilot equipment, and an experimental equation of heat capacity was presented. Because the developed catalyst has higher selectivity than that of ion exchange resins, operation with high concentration of ethylene oxide becomes possible. However, the large reaction heat of operation in an adiabatic reactor causes a severe temperature rise, which can affect product quality. Elimination of reaction heat is necessary to reduce the temperature rise, and utilization of the latent heat of ammonia vaporization is proposed as a solution. A selective monoethanolamine production process with high productivity has been developed by adopting a model of partial vaporization of ammonia and using the modified clay catalyst.

1. Introduction

Ethanolamines are a class of organic compounds that include 2-aminoethanol (MEA), 2,2′-iminodiethanol (DEA), and 2,2′,2″-nitrilotriethanol (TEA). They are important basic chemicals, produced at a global rate of about 1.3 million metric tons per year, and their consumption grows by 4–5% a year. They are versatile chemicals that have the properties of both amines and alcohols. They are used in diverse areas, such as gas sweetening, detergent and specialty cleaner formulations, intermediates for ethyleneamines, agricultural chemicals such as herbicides, urethane foam catalysts, pharmaceuticals, textile processing aids, metalworking, and oil-well rust preventives.

The synthetic method for the production of ethanolamines is shown in Eqs. (1)–(3), and is a typical consecutive reaction with 3 steps.

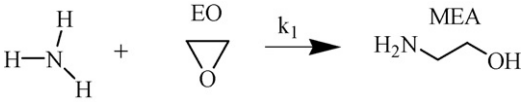

(1)

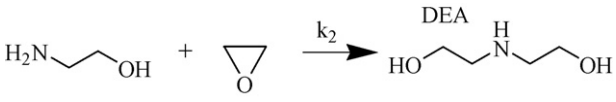

(2)

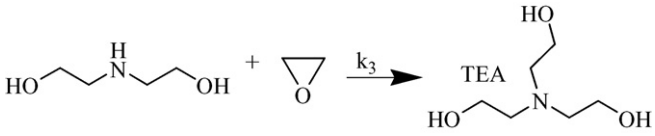

(3)

Currently, ethanolamines are produced on an industrial scale exclusively by the reaction of EO with excess ammonia [1]. The reaction of EO with anhydrous ammonia occurs very slowly and is accelerated by water [2]. The water must be separated from the products, which is energy consuming. This has led to an increasing interest in anhydrous methods using heterogeneous catalysts. Weibull et al. reported the possibility of using ion exchange resins [3]. A potential disadvantage of organic ion exchange resins is their lack of stability at high temperatures. For the requirements of high-temperature stability and the presence of acidic sites, many inorganic solid acids, such as acidic silica–aluminas, zeolites, and acid clays, have been investigated. [4,5]. However, a catalyst that is superior in activity and selectivity to ion exchange resin has not been discovered.

Abbreviations: MEA, monoethanolamine; DEA, diethanolamine; TEA, triethanolamine; EO, ethylene oxide.

* Corresponding author. Tel.: +81 6 6317 2252; fax: +81 6 6317 2992.
E-mail address: hideaki_tsuneki@shokubai.co.jp (H. Tsuneki).

1385-8947/$ – see front matter © 2009 Elsevier B.V. All rights reserved.
doi:10.1016/j.cej.2008.12.031

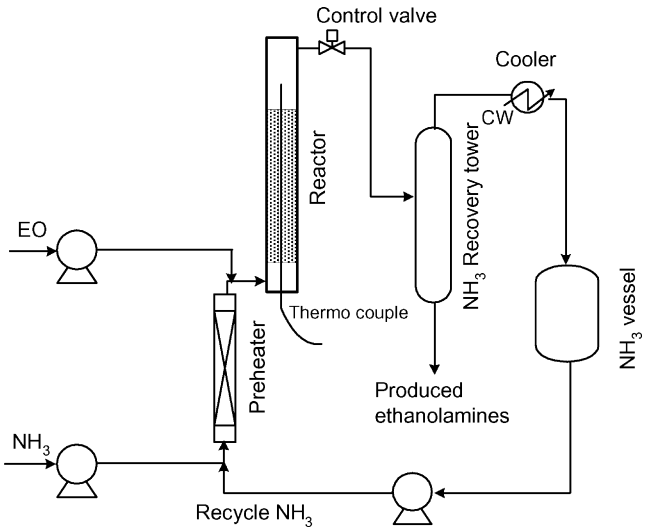

Fig. 1. Flow scheme of pilot equipment. Reactor: 67 mm$^{\phi}$ 2000 mm^{L} Catalyst volume 3–6 L, with thermal insulation material wounded up. Heat liberation is compensated by heating.

To meet increasing demand for MEA, Nippon Shokubai developed a modified clay catalyst with high activity and high selectivity for MEA production [6–9]. The use of this catalyst can raise EO concentration in the reactor inlet and increase process productivity. However, this can cause the problem of a large temperature rise, due to reaction heat in an adiabatic reactor [10]. In this paper, we report on a heat capacity equation for an ammonia–EO–ethanolamine system and present a high-productivity process that uses partial vaporization of ammonia to eliminate reaction heat for reducing the temperature rise in the adiabatic reactor.

2. Experiment

2.1. Catalyst

Catalyst A: Clay modified with rare earth elements [11]. Preparation example: montmorillonite (2 kg) was added to a 0.05 mol/L lanthanum nitrate aqueous solution (0.1 m^3). This slurry was stirred for 12 h and then settled for a further 12 h to precipitate lanthanum ion-exchanged montmorillonite. The precipitate was filtered after eliminating supernatant liquid and rinsed using 0.1 m^3 of ion exchange water. A pore forming agent (2 kg), such as cellulose powder, was added to the resulting cake. An extruder molded the cake in the shape of a string, 0.4 mm in diameter. The molded product was dried at 393 K for 12 h, and granulated to a length of 2–5 mm. The resulting granules were calcined in air at 773 K for 4 h.

Catalyst B: Ion exchange resin. Strongly acidic, gel type (Dowex® 50 W, particle size: 0.3–0.8 mm)

2.2. Equipment

The flow scheme of our pilot system is shown in Fig. 1. Liquid ammonia and EO were fed using high-pressure metering pumps with two heads, one for each chemical. Before entering the reactor, the reactant liquid was preheated.

The reactor consisted of a 2000 mm-long stainless steel tube with an inside diameter of 67 mm. The reactor was highly insulated with ceramic wool, and a heater compensated for the reactor's heat loss. A movable K-type thermocouple measured the temperature profile of the catalyst bed.

A regulating valve placed after the reactor maintained the reactor pressure at the desired level. Most of the excess ammonia was stripped off in a distillation column and recycled to the reactor.

2.3. Reaction conditions

Reaction pressure was controlled at 10–13 MPa. The reactor inlet temperature was controlled in the range of 300–373 K, and the maximum reactor outlet temperature was 430 K. The EO concentration was 2–11.1 mol% (NH_3/EO molar ratio = 50–8). Weight hourly space velocity (WHSV) was controlled at 1–5 h^{-1}.

3. Results and discussion

3.1. Reaction rate equation

In designing a reaction process, it is very important to derive a reaction rate model. From a practical viewpoint, a desired reaction rate model should be sufficiently simple and accurate one enough to explain reaction data. Our reaction model is a simple second-order model. Reaction rate (r_1, r_2, r_3) equations for each step in the reaction scheme are expressed as follows:

$$r_1 = k_1 C_N C_E, \tag{4}$$

$$r_2 = k_2 C_M C_E = k_1 \alpha C_M C_E, \tag{5}$$

$$r_3 = k_3 C_D C_E = k_1 \beta C_D C_E, \tag{6}$$

where C_N, C_E, C_M, and C_D are concentrations of ammonia, EO, MEA, and DEA, respectively. k_1, k_2, and k_3 are reaction rate constants, and α and β are parameters, defined as k_2/k_1 and k_3/k_1, respectively. k_1 is expressed as Eq. (7).

$$k_1 = A_1 \exp\left(\frac{-E_a}{RT}\right), \tag{7}$$

where A_1 and E_a are frequency factor and activation energy of k_1 respectively. R is gas constant. T is reaction temperature. The concentration change rate of each component is expressed as follows:

$$\frac{dC_N}{dt} = -r_1 = -k_1 C_N C_E, \tag{8}$$

$$\frac{dC_M}{dt} = r_1 - r_2 = k_1(C_N - \alpha C_M)C_E, \tag{9}$$

$$\frac{dC_D}{dt} = r_2 - r_3 = k_1(\alpha C_M - \beta C_D)C_E, \tag{10}$$

$$\frac{dC_E}{dt} = -r_1 - r_2 - r_3 = -k_1(C_N + \alpha C_M + \beta C_D)C_E, \tag{11}$$

where t is reaction time. In actual reactor, t at point z of catalyst layer is defined as·WHSV^{-1}·z·$L0^{-1}$, where $L0$ is whole length of catalyst layer.

Let C_{N0} denote initial C_N. Eqs. (12) and (13) are obtained by integrating Eqs. (8)–(11).

$$\frac{C_M}{C_{N0}} = \frac{(C_N/C_{N0})^{\alpha} - C_N/C_{N0}}{1-\alpha}, \tag{12}$$

$$\frac{C_D}{C_{N0}} = \frac{\alpha}{1-\alpha}\left[\frac{C_N/C_{N0} - (C_N/C_{N0})^{\beta}}{1-\beta} - \frac{(C_N/C_{N0})^{\alpha} - (C_N/C_{N0})^{\beta}}{\alpha-\beta}\right], \tag{13}$$

Selectivity for MEA increases when α and β are reduced. These parameters are in the range of 5–7 for the ion exchange resin (Catalyst B) and about 3 for the modified clay (Catalyst A).

3.2. Heat capacity measurement and derivation of experimental equation

The developed catalyst was calcined at high temperature (773 K). Therefore, its heat resistance is higher than that of the ion exchange

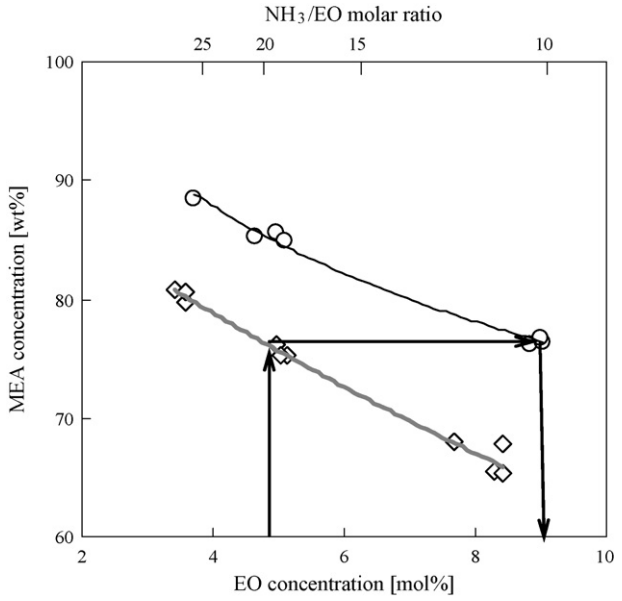

Fig. 2. MEA concentration in produced amines as a function of EO concentration. (○) Catalyst A: Modified clay catalyst. (◊) Catalyst B: Ion exchange resin.

resin (normal use temperature: 393–403 K). As shown in Fig. 2, the selectivity of the catalyst for MEA is improved; thus, the reaction can be executed at high EO concentrations (i.e., low NH_3/EO molar ratio). In this case, the adiabatic temperature rise is a severe problem. The maximum temperature of the reactor is limited to about 430 K to maintain product ethanolamines qualities, such as color.

Fig. 3 shows the relationship between EO concentration and temperature rise observed using the pilot equipment. The reactor was highly insulated, and a heater compensated for heat loss for achieving nearly adiabatic conditions. As shown in Fig. 4, isobaric heat capacity (C_P) of the reaction mixture, estimated by a simple mixing rule, disagreed with observed data.

3.2.1. Isobaric heat capacity estimated by Vamling's equation

Vamling and Cider reported an experimental equation of C_P as a function of pressure (P) and temperature (T) [12].

$$C_P = C_{P,a} + \frac{C_{P,b}}{C_{P,c}^{(13\ \mathrm{MPa})} + dC_{P,c}dP(P - P_0) - T}, \tag{14}$$

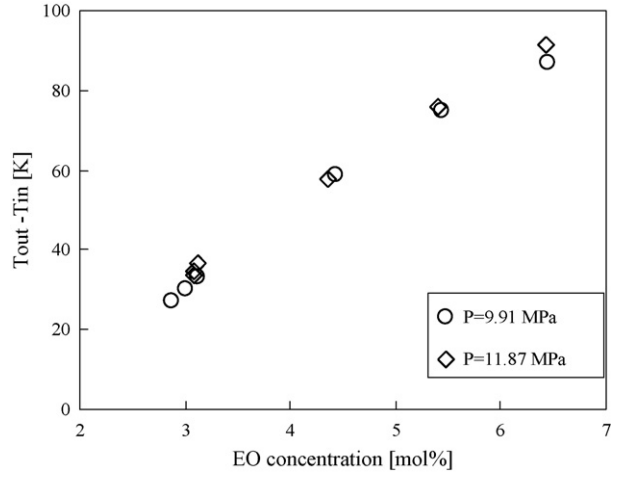

Fig. 3. Temperature rise at various EO concentrations. Catalyst A.

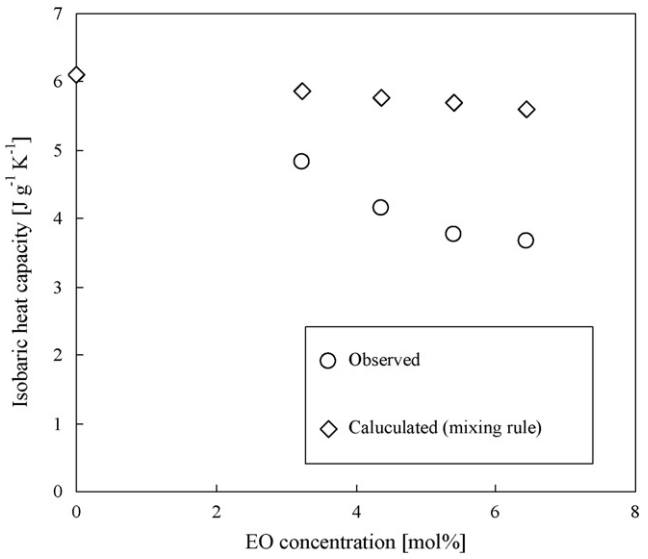

Fig. 4. Effect of EO concentration on isobaric heat capacity. Catalyst A, reaction pressure: 11.87 MPa, heat capacity: average value of reactor inlet and outlet.

where $P_0 = 13 \times 10^6$ Pa and $C_{P,a}$, $C_{P,b}$, $C_{P,c}^{(13\ \mathrm{MPa})}$, and $dC_{P,c}dP$ are parameters.

The values of the parameters in Eq. (14) are given below (some parameters are expressed by the ratio between the parameter and the reaction heat).

$$\frac{-\Delta H}{C_{P,a}} = 31.3 \pm 1.8 \quad (\mathrm{kg\,K/mol}),$$

$$\frac{-\Delta H}{C_{P,b}} = 2.08 \pm 0.56 \quad (\mathrm{kg/mol}),$$

$$C_{P,c}^{(13\ \mathrm{MPa})} = 424.6 \pm 7.4 \quad (\mathrm{K}),$$

$$dC_{P,c}dP = 5.3 \times 10^{-6} \pm 3.8 \times 10^{-6} \quad (\mathrm{K/Pa}).$$

Eq. (14) was derived from experimental data; therefore, agreement between the calculated and observed values was better than that for values calculated using the simple mixing rule (see Table 1). Reactor outlet temperature (T_{out}) is calculated by solving Eq. (15).

$$\int_{T_{\mathrm{in}}}^{T_{\mathrm{out}}} C_{P,a} + \frac{C_{P,b}}{|C_{P,c}^{13\ \mathrm{MPa}} + dC_P dP(P - P_0)|} dT = \Delta H_{\mathrm{R}}, \tag{15}$$

where ΔH_{R} ($\mathrm{J\,g^{-1}}$) is the reaction heat of 1 g of reaction mixture, and T_{in} is the reactor inlet temperature.

Eq. (14) does not involve an EO-concentration term; however, EO concentration affected C_P considerably, as shown in Figs. 3 and 4. The differences between calculated and observed values are shown in Fig. 5A. When the EO concentration is low, the estimated heat capacity is too small, and as a result, the calculated outlet temperature becomes high. On the contrary, when EO concentration is high, the outlet temperature becomes low.

3.2.2. Revised Vamling's equation

If an EO-concentration term is taken into consideration, a revised Vamling's equation can express the actual heat capacity with higher accuracy. Figs. 4 and 5A show that the EO-concentration term has an exponential effect. An EO-concentration term is necessary in the denominator of the 2nd term, because EO concentration affects the

Table 1
Effect of EO concentration on isobaric heat capacity.

EO concentration (mol%)	Pressure (MPa)	T_{inlet} (K)	T_{outlet} (K)	Heat capacity (J g^{-1})	Calculated T_{outlet} (K)	Calculated heat capacity* (J g^{-1})	Error (K)
2.87	9.91	371.8	399.0	5.856	406.3	5.740	7.3
3.00	9.91	362.7	392.6	5.555	400.9	5.192	8.3
3.13	9.91	354.1	387.1	5.279	395.5	4.871	8.5
4.44	9.91	344.0	401.2	4.207	401.4	4.572	−1.3
5.44	9.91	330.6	405.4	3.885	401.5	4.258	−3.9
6.44	9.91	319.0	406.0	3.893	402.7	3.952	−3.3
3.08	11.87	374.3	408.0	5.053	409.8	5.190	1.8
3.09	11.87	353.6	388.3	4.919	394.7	4.581	6.4
3.13	11.87	343.5	380.1	4.726	386.8	4.427	6.7
4.36	11.87	345.2	403.2	4.082	401.5	4.288	−1.6
5.40	11.87	329.5	405.5	3.797	400.3	3.969	−5.1
6.43	11.87	318.9	410.2	3.705	402.5	3.770	−7.6

Catalyst A, calculated heat capacity.
* Valming's equation (Eq. (14)).

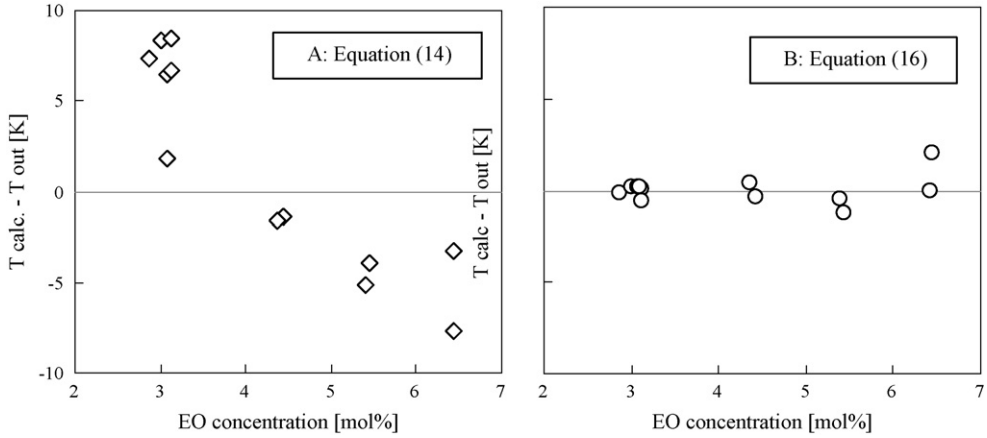

Fig. 5. Evaluation of heat capacity equations. Catalyst A, (A) Vamling's equation (14). (B) Revised Vamling's equation (16).

critical condition. Thus, the empirical formula is revised as follows:

$$C_P = C_{P,a} + a\exp(cC_E) + \frac{C_{P,b}}{C_{P,c}^{(13\,\mathrm{MPa})} + bC_E + dC_{P,c}dP(P - P_0) - T}, \quad (16)$$

where C_E is the EO concentration (mol%), and a, b, and c are additional parameters for Eq. (14).

$$\int_{T_{in}}^{T_{out}} C_{P,a} + a\exp(cC_E) + \frac{C_{P,b}}{|C_{P,c}^{13\,\mathrm{MPa}} + bC_E + dC_P dP(P - P_0)|}dT = \Delta H_R, \quad (17)$$

Parameters (a, b, and c) were determined using the nonlinear least-squares method to satisfy Eq. (16). The obtained parameters are shown below.

$$\frac{-\Delta H}{C_{P,a}} = 29.38 \quad (\mathrm{kg\,K/mol})$$

$$\frac{-\Delta H}{C_{P,b}} = 1.871 \quad (\mathrm{kg/mol})$$

$$C_{P,c}^{(13\,\mathrm{MPa})} = 453.8 \quad (\mathrm{K})$$

$$dC_{P,c}dP = 2.0 \times 10^{-5} \quad (\mathrm{K/Pa})$$

$$\frac{-\Delta H}{a} = 1.798 \quad (\mathrm{kg/K\,mol})$$

$$b = 14.07 \quad (\mathrm{K/mol\%})$$

$$c = -1.2845 \quad (\mathrm{mol\%^{-1}})$$

The differences between observed and calculated values are shown in Fig. 5B. By introducing an EO-concentration term, the errors in Fig. 5B show a considerable decrease compared to those in Fig. 5A.

Using this heat capacity, temperature rise rate is expressed by Eq. (18).

$$\frac{dT}{dt} = (r_1 + r_2 + r_3)\frac{\Delta H}{C_P} = \frac{k_1(C_N + \alpha C_M + \beta C_M)C_E\Delta H}{C_P}, \quad (18)$$

The temperature profile of the catalyst bed is obtained by integrating the differential system from Eqs. (8)–(11) and (18). Some examples of observed data and calculated values are shown in Fig. 6. The calculated values agree well with observed data.

3.3. Suppression of temperature rise in an adiabatic reactor—ammonia partial vaporization

When EO concentration was increased above 7 mol% at relative low reaction pressure, the observed heat capacity was larger than that calculated using Eq. (16). Table 2 shows the observed and calculated heat capacities, reactor outlet temperature, and error. Fig. 7A shows temperature profiles at various EO concentrations, and Fig. 7B compares the observed and calculated values at an EO concentration of 9.18 mol%. Though the reaction heat increased with EO concentration, the observed temperature rise was smaller

Table 2
Effect of EO concentration on apparent heat capacity at high EO concentration.

EO concentration (mol%)	Pressure (MPa)	T_{inlet} (K)	T_{outlet} (K)	Heat capacity (J g^{-1})	Calculated T_{outlet} (K)	Calculated Heat capacity (J g^{-1})	Error (K)
7.14	9.91	319.2	412.7	4.086	419.6	3.348	6.9
7.20	10.40	319.8	414.0	3.977	421.5	3.334	7.5
7.80	9.91	319.8	412.7	4.312	430.0	3.297	17.3
9.18	9.91	320.5	415.8	4.893	443.8	3.780	28.0

Catalyst A.

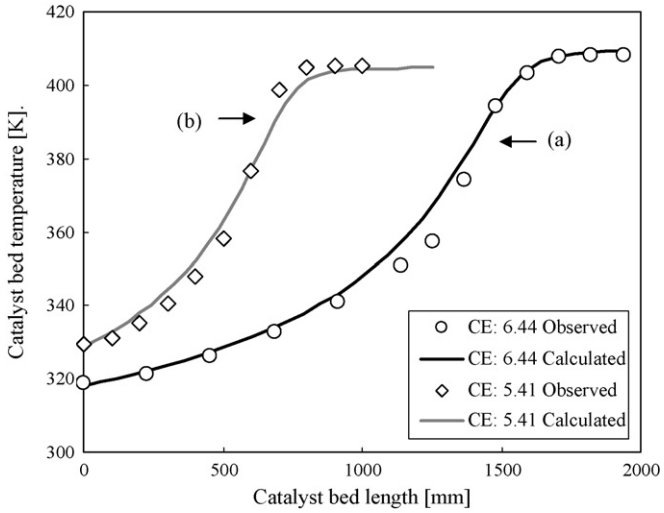

Fig. 6. Calculated and observed temperature profile. Catalyst A, reaction pressure 11.87 MPa, (a) C_E: 6.44 mol%, inlet temperature 319.2 K, WHSV 3.8 h^{-1} (NH_3/EO molar ratio 14.5). (b) C_E: 5.41 mol%, inlet temperature 338.2 K, WHSV 3.2 h^{-1} (NH_3/EO molar ratio 17.5).

than expected. In the case of condition (a) in Fig. 7A, the temperature profile line curved gently at the inflection point, whereas for conditions (b) and (c), it curved sharply. The calculated value in Fig. 7B agreed with the observed data up to the inflection point.

This phenomenon is considered to be due to the relative low reaction pressure. The reaction mixture reaches its boiling point and a part of the ammonia vaporizes because it receives latent heat from the reaction mixture, and the temperature rise is restrained. Therefore, when ammonia vaporization begins, the temperature rise stops suddenly, and the temperature profile curve bends sharply. If the boiling point and apparent heat capacity of the reaction mixture could be estimated, the temperature profile for high EO concentrations could be predicted. When the EO concentration is increased to achieve high productivity, the temperature rise of the reaction mixture can be suppressed by control of the reaction pressure Thus, concerns over quality deterioration decrease.

3.3.1. *Estimation of apparent heat capacity on vaporization of ammonia*

The boiling point and apparent heat capacity of the reaction mixture are estimated by the following procedure:

(1) Integrate the reaction rate Eqs. (8)–(11) and (18) without considering ammonia vaporization, and determine the temperature profile and the distribution of reaction mixture composition.
(2) Calculate equilibrium vapor pressure of the reaction mixture at each point from the composition.
(3) Determine a point where equilibrium vapor pressure equals reaction pressure; this is the boiling point.
(4) Estimate the latent heat of ammonia vaporization at the boiling point.
(5) Estimate the quantity of ammonia vaporized based on fact that the reaction heat that of all of the unreacted EO at the boiling point is used for the reaction.
(6) Calculate the temperature and composition at the point the reaction terminates.
(7) Estimate the latent heat of ammonia vaporization at the reaction termination point; then, use this value to correct the quantity of ammonia vaporized and the temperature at the reaction termination point.
(8) Determine the apparent heat capacity based on the boiling point, the reaction termination point, and the reaction heat evolution.
(9) Integrate the reaction rate equations using this apparent heat capacity after the boiling point, and determine the temperature profile and the distribution of the reaction mixture composition.

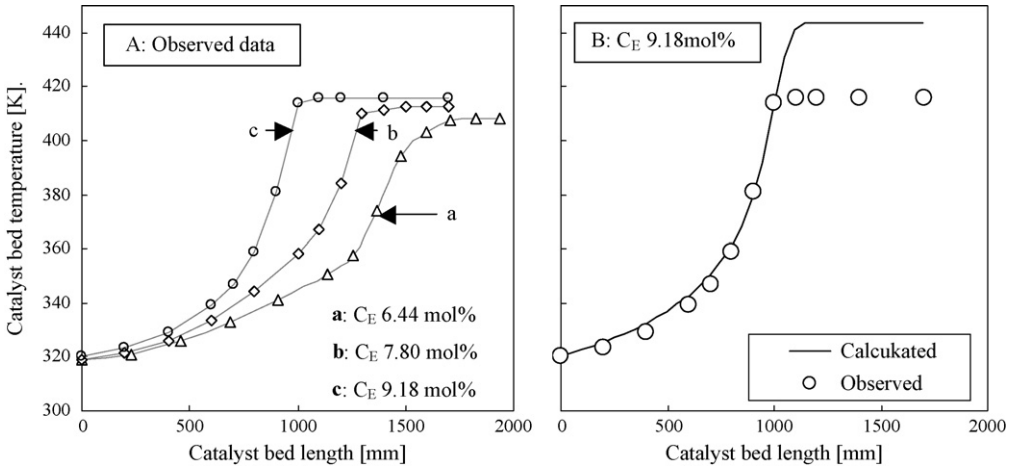

Fig. 7. Temperature profile at high EO concentration. Catalyst A (A) Observed data, (a) C_E 6.44 mol%; pressure 11.87 MPa, WHSV 3.8 h^{-1}. (b, c) C_E 7.80 and 9.18 mol%; pressure 9.91 MPa, WHSV 3.2–3.4 h^{-1}. (B) Comparison between observed data and calculated profile at C_E 9.18 mol%.

Because of lacking the values of various properties are unknown, many assumptions are necessary to estimate these values when using this procedure.

3.3.2. Estimation of equilibrium vapor pressure of reaction mixture

The first problem is estimating the vapor pressure of ammonia. Vapor pressure is not defined above the critical temperature of ammonia (405.6 K), because saturated liquid does not exist in that region. Therefore, it is necessary to postulate the vapor pressure of ammonia. Vapor pressure data is available up to the critical temperature; hence, the postulated vapor pressure above the critical temperature can be defined by a linear extrapolation of the available data.

The second problem is estimating the activity coefficient of ammonia. If the coexistence of EO and ethanolamines at high pressure is taken into account, the partial pressure of ammonia is not proportional to its mole fraction. The vapor pressure of the reaction liquid (P_R) is presented in Eq. (19) using the correction coefficient (fv) of ammonia activity.

$$P_R = fv P_{NH_3} x_{NH_3} + P_{EO} x_{EO} + P_{MEA} x_{MEA} + P_{DEA} x_{DEA} + P_{TEA} x_{TEA}, \quad (19)$$

where P and x are the vapor pressure and mole fraction of each component, respectively. The value of fv becomes 0.87 from the boiling point data of NH_3/EO at molar ratios of 10 and 12.

3.3.3. Estimation of latent heat of ammonia vaporization

The latent heat of ammonia vaporization cannot be determined directly at temperatures above the critical temperature. In general, the latent heat of vaporization is estimated using the Watson relation (20).

$$H_2 = H_1 \left(\frac{\left(1 - \frac{T_2}{T_C}\right)}{\left(1 - \frac{T_1}{T_C}\right)} \right)^n, \quad (20)$$

where T_c is the critical temperature, and H_i is the latent heat at temperature T_i. The critical temperature of a reaction mixture containing EO and ethanolamines is considerably higher than that of ammonia. Eq. (20) can be applied to the reaction mixture using the estimated critical temperature. A value of $n = 0.38$ is generally used in this equation. When the critical temperature of the reaction mixture is T_{cm}, the latent heat of vaporization of the reaction mixture (H_v) at temperature T is calculated in Eq. (20), using $H_1 = 665.7\ J\ g^{-1}$ at $T_1 = 377.6$ K (from latent heat data of ammonia).

$$H_v = 665.7 \left(\frac{(1 - T/T_{Cm})}{0.06903} \right)^{0.38}, \quad (21)$$

Eq. (22) is used to estimate the critical temperature T_{cm} of the reaction mixture.

$$T_{cm} = \sum_i \sum_j \phi_i \phi_j T_{cij}, \quad (22)$$

where ϕ and T_{cij} are estimated by Eqs. (23) and (24), respectively.

$$\phi_i = \frac{x_i V_i}{\sum_j x_j V_j}, \quad (23)$$

$$T_{cij} = \sqrt{T_{ci} T_{cj}}, \quad (24)$$

where x_i, V_i, and T_{ci} are the mole fraction, critical volume, and critical temperature of the ith component, respectively.

3.3.4. Simulation of temperature profile using model of ammonia partial vaporization

According to simulations using this model of ammonia partial vaporization, considerable suppression of temperature rise is expected at high EO concentrations, such as 11.1 mol%. Fig. 8 shows (1) values calculated using this model and the observed data, and (2) the entire temperature profile of the catalyst bed. Without ammonia partial vaporization, the catalyst bed outlet temperature becomes 465 K, hence raising concerns about product qualities, such as coloration.

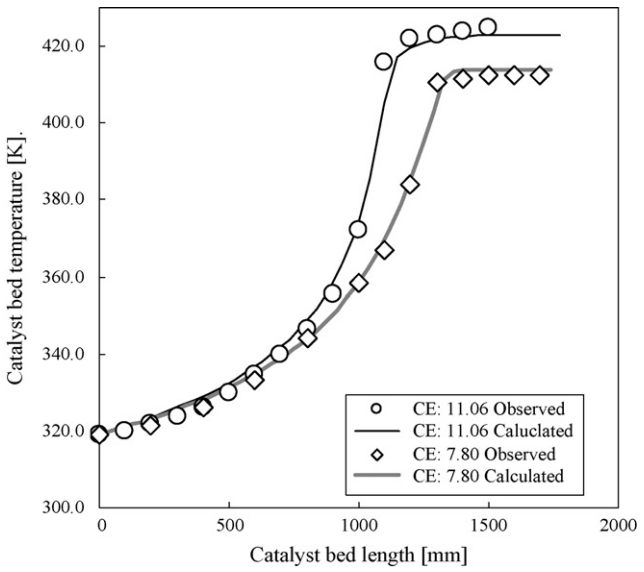

Fig. 8. Temperature profile at extreme high EO concentration condition. (○) C_E 11.06 mol%, (◊) C_E 7.80 mol%, Catalyst A, WHSV: 3.4–3.75 h^{-1}, pressure 9.91 MPa,

Fig. 9 shows the unreacted quantity of ammonia and EO for initial EO = 1. A considerable quantity of ammonia, much more than that consumed by the reaction, is lost by vaporization from the reaction mixture. In the case of high EO concentration, as shown in Fig. 9, the quantity of ammonia vaporization is 45%, and the concentration of ammonia in the reaction mixture decreases considerably. Therefore, the quantity of monoethanolamine formed by the reaction between ammonia and EO decreases slightly. Table 3 shows the product distribution data and the calculated values at various EO concentrations. Comparing entry 1, where there is no ammonia vaporization, with entry 4 shows good agreement between observed and calculated values. Comparing entries 2, 5, and 8

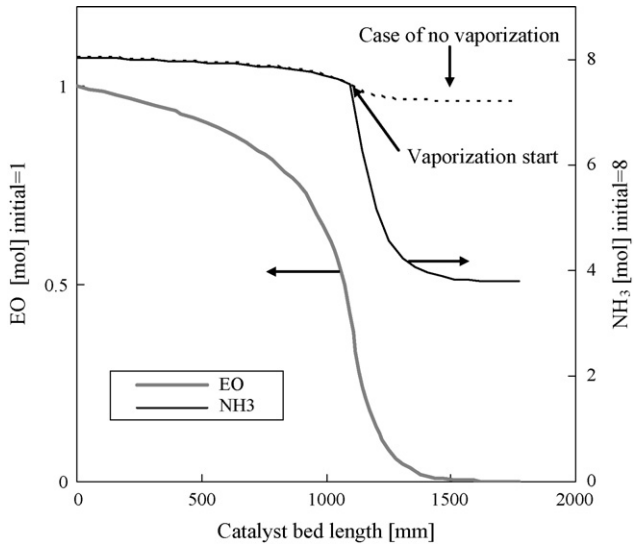

Fig. 9. Calculated NH_3 and EO distribution in the reaction liquid at ammonia partial vaporization condition. C_E 11.04 mol% (NH_3/EO molar ratio 8), Catalyst A, WHSV 3.75 h^{-1}, pressure 9.91 MPa.

Table 3
Product distribution change at ammonia partial vaporization condition.

Entry	NH_3/EO molar ratio	Products distribution (wt%)			Vaporized ammonia (%)	
		MEA	DEA	TEA		
1	14.6	84.70	14.26	1.04		Observed data
2	12.0	80.74	17.66	1.66		
3	8.0	69.8	26.4	3.8		
4	14.6	84.11	14.77	1.11		Calculated value without vaporization
5	12.0	81.29	17.13	1.59		
6	8.0	74.24	22.68	3.05		
7	14.6	84.11	14.77	1.11	–	Calculated value with vaporization
8	12.0	81.16	17.25	1.58	9.6	
9	8.0	70.88	25.33	3.78	45.8	

Catalyst A, reaction pressure 9.91 MPa, WHSV 3.4–3.75 h^{-1},kinetic parameters: α 3.2, β 2.4.

Table 4
Comparison of calculated ethanolamines productivities at various conditions.

Catalyst	EO concentration (mol%)	Reaction pressure (MPa)	T_{inlet} (K)	T_{outlet} (K)	MEA (wt%)	Productivity	
						EAs production rate (kg L^{-1} h^{-1})	Produced EAs/recycled NH_3
B	3.77	12.8	353.2	403.1	80.1	0.47	0.141
B	6.67	12.8	298.2	403.2	70.3	0.22	0.259
A	6.67	12.8	328.2	423.0	83.5	0.69	0.267
A*	6.67	9.9	343.2	413.7	83.0	1.31	0.266
A*	11.05	9.9	318.2	423.5	70.0	0.64	0.478

Catalyst A: modified clay, Catalyst B: ion exchange resin.
* With ammonia partial vaporization.

shows that slight vaporization of ammonia scarcely affected product distribution. However, comparing entry 3, which had severe ammonia vaporization, with entry 6, shows considerable disagreement in product distribution. However, comparing entries 3 and 9 shows that the observed data and calculated values agree within an acceptable range. This means that this model of ammonia partial vaporization can explain not only the temperature profile but also product distribution.

Table 4 shows ethanolamine productivities calculated for various conditions (catalyst type, EO concentration, and with and without ammonia vaporization). In the case of the ion exchange resin, the maximum temperature is limited by its heat resistance temperature, and this also limits EO concentration and productivity. For ammonia vaporization, productivity is higher because of the high EO concentration. A highly monoethanolamine-selective process with high productivity is realized using a modified clay catalyst and an ammonia partial vaporization process.

4. Conclusion

Accurate temperature profile data were obtained using the pilot equipment that was packed with the clay catalyst modified with rare earth elements. Revised experimental equations for evaluating the isobaric heat capacity of the ammonia–EO–ethanolamines system have been proposed based on this data, and a simulation model that explains the temperature profile in an adiabatic reactor was presented. In the case of high EO concentrations at relatively low reaction pressure, the initial model cannot explain the temperature profile. When the model is revised by considering ammonia partial vaporization, it demonstrates that reaction heat can be eliminated from an adiabatic reactor using the latent heat of ammonia vaporization. Thus, a catalytic ethanolamine production process with high productivity and without concerns of deterioration of product quality has been realized.

Acknowledgment

The authors thank the staff of the Nippon Shokubai Kawasaki plant for their contribution to the operation of the pilot equipment.

References

[1] M.R. Edens, J.F. Lochary, Kirk-Other Encyclopedia of Chemical Technology, vol. 2, John Wiley & Sons, New York, 1991, pp. 8–9.
[2] M. Miki, T. Ito, M. Hatta, T. Okabe, Yukagaku 15 (1966) 215–220.
[3] B.J.G. Weibull, L.U.F. Folke, S.O. Lindstrom, US Patent 3697598 (1972).
[4] Jr. Johnson, L. Fred, U.S. Patent 4,438,281 (1984).
[5] J.N. Grice, J.F. Knifton, U.S. Patent 4,939,301 (1990).
[6] A. Moriya, H. Tsuneki, JP Patent 2771465 (1998).
[7] A. Moriya, H. Tsuneki, Shokubai 38 (1996) 91.
[8] H. Tsuneki, Shokubai 40 (1998) 304–309.
[9] H. Tsuneki, M. Kirishiki, T. Oku, Bull. Chem. Soc. Jpn. 80 (2007) 1075–1090.
[10] H. Tsuneki, A. Moriya, JP Patent 2996914 (1999).
[11] A. Moriya, H. Tsuneki, JP Patent 2773485 (1998).
[12] L. Vamling, L. Cider, Ind. Eng. Chem. Prod. Res. Dev. 25 (1986) 424–430.